All-solid-state Flexible Supercapacitors Based on Screen-printed Graphene Electrodes

Ya Ling Li[1,2,3], *Peng Cheng Li*[1], *Bi Jian Li*[1], *Meng Ke Gao*[1], *Fu Yan Zhao*[1], *Lei Shao*[2,3],
Jian Feng Chen[2,3,*], *Lu Hai Li* [1*]

[1] Beijing Engineering Research Center of Printed Electronics, Beijing Institute of Graphic
Communication, Beijing 102600, PR China
[2] Research Center of the Ministry of Education for High Gravity Engineering and Technology, Beijing
University of Chemical Technology, Beijing 100029, PR China
[3] State Key Laboratory of Organic–Inorganic Composites, Beijing University of Chemical Technology,
Beijing 100029, PR China
[*]E-mail: liluhai@bigc.edu.cn, chenjf@mail.buct.edu.cn

Graphene ink was produced using graphene, polyvinylidene fluoride, and acetylene black with 1-methyl-2-pyrrolidinone in a ball mill and the thickness and viscosity of the ink were characterized. Afterwards, the conductive silver ink was screen printed and thermally cured onto a poly(ethylene terephthalate) substrate. In addition, the prepared graphene ink was screen-printed onto the conductive silver layer and dried to create a flexible supercapacitor electrode. A PVA-H_2SO_4 gel was coated onto the flexible electrode as electrolyte. Finally, a symmetric supercapacitor was successfully assembled and shows a specific capacitance of 190.6 F g^{-1} at 0.5 A g^{-1} and a maximum energy density of 16.94 W h kg^{-1}. The three devices connected in series to light up a light-emitting diode. The printed flexible electrodes created using a simple process could play an important role in the energy storage field.

1. INTRODUCTION

All-solid-state flexible supercapacitors occupy a prominent position in energy storage systems and have a promising application in wearable electronics and flexible printed electronics. [1-2] The flexible electrode, gel electrolyte and porous separator have a large influence on the electrochemical performance of supercapacitors. Various fabrication methods for flexible supercapacitor electrodes have been reported such as spray coating [3] and spin-coating techniques, filtering the conductive and active materials onto paper, [4] electrophoretic deposition on carbon cloth [5], magnetron sputtering

combined with electrodeposition method [6] and others. However, these methods for making supercapacitor electrodes are complex and expensive. Printed electronics have the merits of low cost, large area and roll-to-roll or the fabricating of electronic devices. Luhai Li et al have performed work on printing electronics and have acquired high quality conductive inks and flexible conductive films. [7-9] Therefore, we adopted a the printing technology to create flexible supercapacitor electrodes. Among the printing techniques, the screen-printing method is a convenient and effective method to acquire specific patterns and thicknesses on a large-scale flexible substrate [10-11] Here we used the technique to fabricate supercapacitor electrodes including the current collector and active electrodes on a poly(ethylene terephthalate) (PET) substrate using commercial conductive silver paste and a homemade graphene active materials paste.

Carbon materials such as active carbon (AC) and graphene are commonly used as active electrode materials in electric double layer capacitance (EDLC) supercapacitors due to their large surface area, controllable pore size distribution and good cycling performance. Above all, graphene electrode high conductivity has great potential for energy harvesting and storage in solar cells, fuel cells, batteries and supercapacitors. [12-15] In this work, we explored a graphene ink formulation and presented a facile method to fabricate a flexible supercapacitor electrode using printing technology. In addition, a symmetric supercapacitor was assembled using two pieces of the above flexible electrodes and separating them with a separator using a PVA-H_2SO_4 gel as the electrolyte. The electrochemical properties of the device were studied. We explored a simple and quick approach to make a supercapacitor electrode using screen printing technology and the method has a wide application for energy devices.

2. EXPERIMENTAL

2.1 Materials

Graphene was purchased from the Six Element (Changzhou) Materials Technology Co, Ltd. The conductive silver paste (BY-2000) was purchased from Shanghai Baoyin Electronic Materials Ltd. H_2SO_4 was purchased from Sinopharm Chemical Reagent Co., Ltd. PVA-124 was purchased from Aladdin Chemistry Co., Ltd. All chemicals were used as received. Acetylene black, polyvinylidene fluoride (PVDF, HSV900, ARKEMA), N-methylpyrrolidone (NMP, > 99.9%), and the membrane (TF4030, NKK) were purchased locally. The polyethylene terephthalate (PET) film with a one-sided hydrophilic coating was supplied by the China Lucky Group Corp. The graphene powder was characterized by a surface area & pore size analyser (Quadrasorb SI, Quantachrome Instruments) and a Raman spectrometer (LabRAM, Horiba Jobin Yvon).

### 2.2 Preparation of the graphene ink and PVA-H_2SO_4 gel

The screen-printed graphene ink was prepared by mixing the graphene (6 g), PVDF (0.75 g) and acetylene black (0.75 g) with amount of NMP and grinding the mixed materials using planetary

ball mill (PM 0.4L, Droide Instrument & Equipment (Shanghai) Co., Ltd) with zirconia beads for six hours. To meet the requirements of screen printing, the viscosity of the paste was measured with a rheometer (ARES, TA Instruments) and the measuring temperature was controlled using Hakke K10 instrument (Thermo Electron Corp., Germany) in the range of 25 ± 0.1 °C.. The fineness was tested using a scraper fineness test.

A PVA-H_2SO_4 gel was used as the solid electrolyte [16]. Briefly, 10 g of H_2SO_4 was placed into 100 ml of de-ionized water, and 10 g of PVA was added into the sulfuric acid solution. The above mixture was stirred at 85 °C until a clear solution formed and then the solution was allowed to stand without stirring at the same temperature in a water bath.

2.3 Fabrication of the all-solid-state flexible supercapacitors

The fabrication process of the solid-state supercapacitor is shown in Fig. 1.
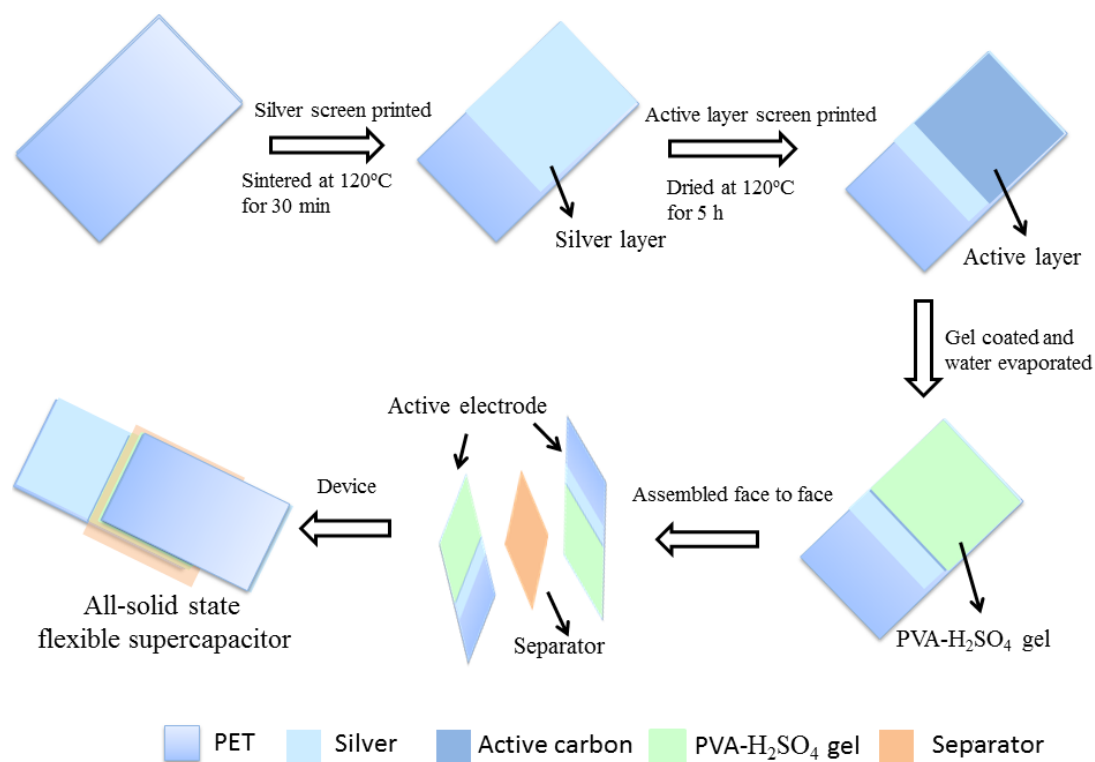
Figure 1. Schematic diagram illustrating the design of the symmetric supercapacitor device.

First, the conductive silver paste was screen printed onto the PET substrate with a 300 mesh nylon printing plate using an automatic screen-printing machine (OS-300FV, OLAT) and then, the paste was dried at 120 °C for 30 min in an electronic oven. The silver electrode was used as the current collector electrode. Second, the as-prepared graphene ink was manually printed onto the silver layer 2.5 cm ×2.5 cm and dried at 120 °C for approximately five hours. Thus the flexible electrodes

including the current collector electrode and active electrode were obtained. In addition, third, the PVA-H_2SO_4 electrolyte was dropped onto the surface of the graphene active electrode and spread out using a capillary tube. Then, the electrodes with the PVA-H_2SO_4 gel were maintained at room temperature overnight to volatilize the water. Finally, the two as-prepared electrodes were placed face to face and separated by a piece of the separator.Then the device was pressed using a pressure of 0.25 MPa from an infrared tablet press. The average mass of the graphene in each electrode was 2.56 mg.

2.4 Electrochemical measurements

All the electrochemical tests were conducted on an AUTOLAB PGSTAT302N potentiostat galvanostat. The cyclic voltammetry (CV), galvanostatic charge/discharge (GCD) and electrochemical impedance spectroscopy (EIS) were performed using a two-electrode system. The EIS was characterized at an open circuit potential in the frequency range from 10^5 Hz to 0.01 Hz with an amplitude of 10 mV. The GCD curves were tested at different current densities of 5, 3, 2, 1 and 0.5 A g^{-1} in the cut off potential range from 0 to 0.8 V. The specific capacitance (C_d, F g^{-1}) of the supercapacitor device was a quarter of that of the specific capacitance (C_{sp}) of the electrode. The specific capacitance, the power density (P, kW kg^{-1}), and energy density (E, W h kg^{-1}) of the supercapacitor device were calculated from the GCD curve using Eq.(1) to Eq.(3): [17-19]

$$C_d = (1/4)C_{sp} = (1/2)(I \times \Delta t)/(m \times \Delta V)$$
(1)

$$E = (1/2)C_d \times (\Delta V)^2 /3.6$$
(2)

$$P = E/\Delta t \times 3600$$
(3)

where I/m (A g^{-1}) is the discharge current density based on the average mass of the graphene in each electrode, Δt (s) is the discharge time corresponding to the cell voltage after excluding the IR drop and ΔV (V) is the applied potential window.

3. RESULTS AND DISCUSSION

3.1 Characterization of the graphene, printed graphene electrode and graphene ink

Fig. 2 shows the N_2 adsorption-desorption isotherm (inset: pore size distribution of graphene) and the Raman spectrum of the graphene. The graphene has a high specific surface area of 2492.4 m^2 g^{-1}, which was calculated using the multi-point BET method. The specific surface area was smaller than the theoretical value of 2630 m^2 g^{-1}, which was due to the re-aggregation of the graphene sheets. [20] The pore size distribution was calculated with N_2 at 77K on carbon (slit/cylindrical pore NLDFT equilibrium model). The graphene has a mesoporous microstructure with the most probable pore diameter of 4.9 nm and a total pore volume of 1.8 cc g^{-1}.
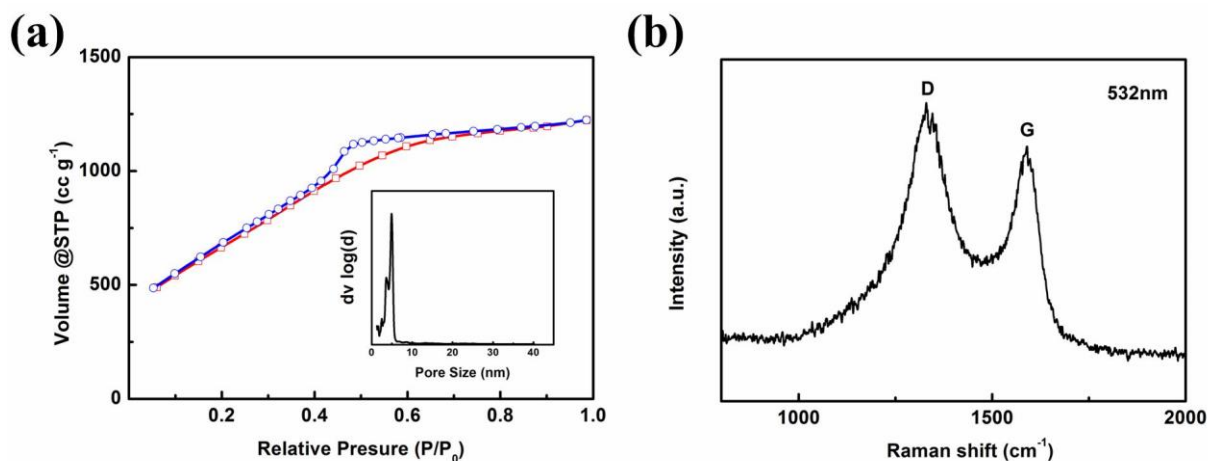
Figure 2. (a) N_2 adsorption-desorption isotherm (inset: pore size distribution of graphene) and (b) Raman spectrum of graphene.
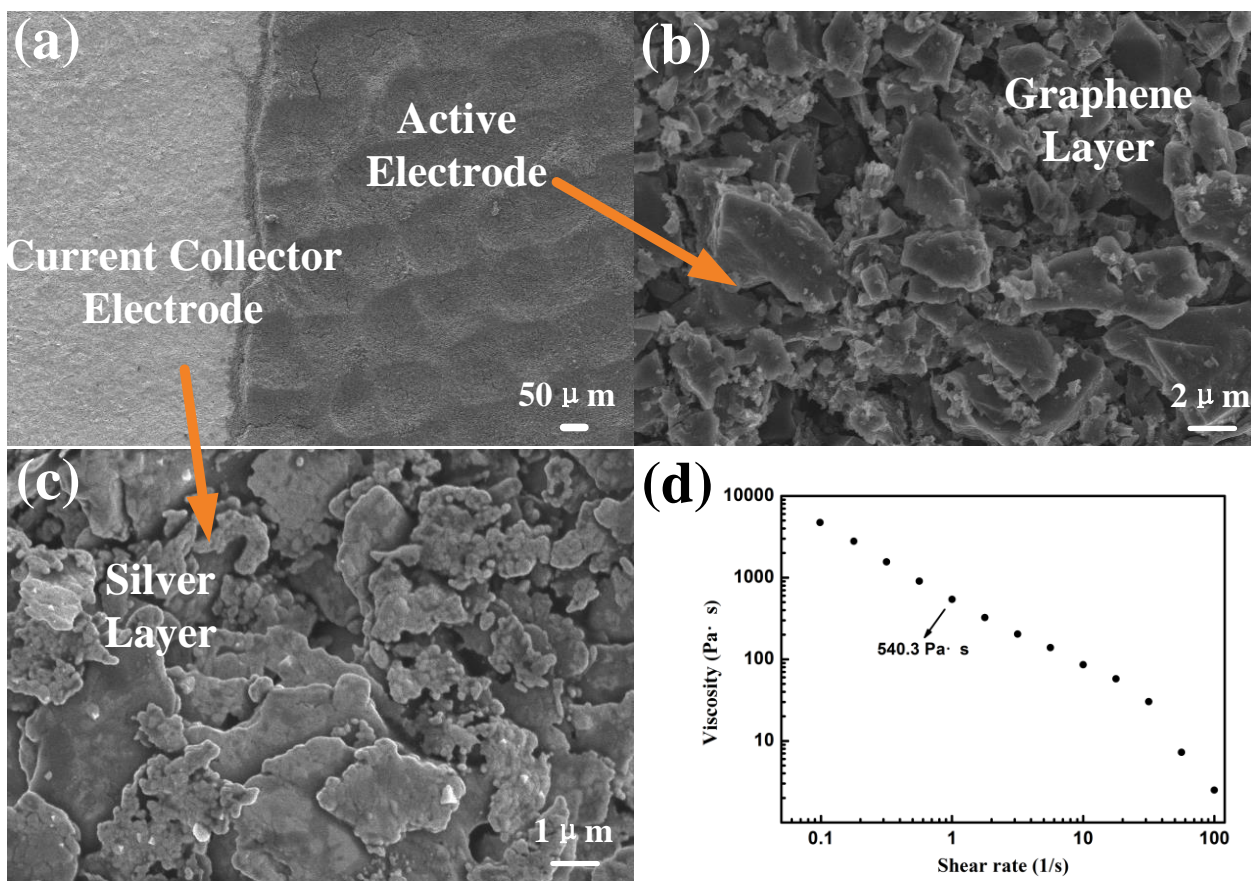
Figure 3. SEM images of (a) the screen printed electrode, (b) graphene layer and (c) silver layer of the electrode; (d) viscosity curve of the graphene ink

The D band at 1333 cm^{-1} and the G band at 1587 cm^{-1} for graphene as shown in Fig. 2b, correspond to the breathing mode of A_{1g} and the in-plane bond-stretching motion of E_{2g} for the sp^2 carbon atoms, respectively. The shift in the D band peak towards lower wavenumbers compared to the

reported values and the large peak intensity ratio (I_D/I_G) of 1.22 demonstrate that the graphene has obvious defects and disorder which can provide more active sites. [20-23]

Fig. 3 shows the morphology of the screen-printed supercapacitor electrode and the viscosity of the graphene ink. The surface of the current collector electrode (Fig. 3a and Fig. 3c) was smooth and the silver particles aggregated together after they were thermally cured at 120 °C. The square resistance of the conductive silver layer was 50 mΩ/□. In Fig. 3a, the rough surface of the graphene active electrode formed because the ink printed onto the substrate adhered to the silk of the screen plate during the separation process. Nevertheless, the special surface structure increased the contact area between the electrolyte and the electrode. The particles in the graphene ink as shown in Fig. 3b, were relative large and there were gaps between the particles. The electrolyte gel could easily infiltrate the graphene electrodes [24] and fully contact the surface of the particles. Fig. 3d shows the graphene ink has a high viscosity of 540.3 Pa·s at a shear rate of 1 s^{-1}. The viscosity decreased with the increasing shear rate, which suggested a unique shear thinning behaviour of the non-Newtonian fluid. To acquire a relatively high mass loading of the active material in a supercapacitor electrode, and to ensure the pintable properties, the viscosity is an important parameter. The viscosity of the ink can be tuned by changing the NMP content in the formulation. The fineness of the graphene ink was less than 10 μm.

3.2 Electrochemical performance of the supercapacitor

Fig. 4a shows the cyclic voltammetry (CV) plots at scan rates of 5-100 mV s^{-1} and Fig. 4b shows the galvanostatic charge/discharge curves at various current densities of 0.5-5 A g^{-1}. No redox peaks were observed in the CV curves and no platform was observed in the charge-discharge curves of the symmetric supercapacitor, which demonstrated the electrical double-layer capacitance of the graphene electrode. In Fig. 4c, the specific capacitance was 190.6 F g^{-1} at 0.5 A g^{-1} and decreased to 100 F g^{-1} at a current density of 5 A g^{-1}. The capacitance retention rate retained 52.5% of its initial capacitance at a large current density. The electrochemical performance of the all-solid-state supercapacitor based on the screen-printed electrodes and other supercapacitors with a similar structure are summarized in Table 1. Table 1 shows that the supercapacitor based on the screen-printed electrodes has a superior electrochemical performance.

Table 1. Comparison of the supercapacitor based on screen-printed graphene electrode and other similar supercapacitors

| Electrode material	Electrode fabrication method	Electrolyte	Specific capacitance (F g^{-1})	Ref.
Graphene	screen printing	PVA-H$_2$SO$_4$	190.6	This work
Porous graphene	electrophoretic deposition	PVA-H$_2$SO$_4$	79.19	[25]
rGO	electrophoretic deposition	PVA-H$_3$PO$_4$	86	[24]
rGO	electrophoretic deposition	PVA-H$_3$PO$_4$	150	[26]

The Ragone plot is shown in Fig. 4d and the symmetric supercapacitor exhibited promising characteristics with a maximum energy density of 16.94 W h kg^{-1} at a power density of 400 W kg^{-1}. The energy density was still 8.89 W h kg^{-1} at a large power density of 4000 W kg^{-1}, which is higher than the previously reported value [24]. Fig. 4e shows the Nyquist plot of the device and the intercept on the x-axis indicated an equivalent series resistance of 0.5 Ω. The low ohmic resistance was due to the full contact among the printed conductive film, printed active layer and electrolyte gel. The supercapacitor retained 68.3% of its initial capacitance after 250 charge/discharge cycles at a current density of 2 A g^{-1} as shown in Fig. 4f. The cycling stability of the device can be improved by encapsulating the device to prevent the degradation of the electrolyte gel and by exploring new types of electrolyte gels [27].
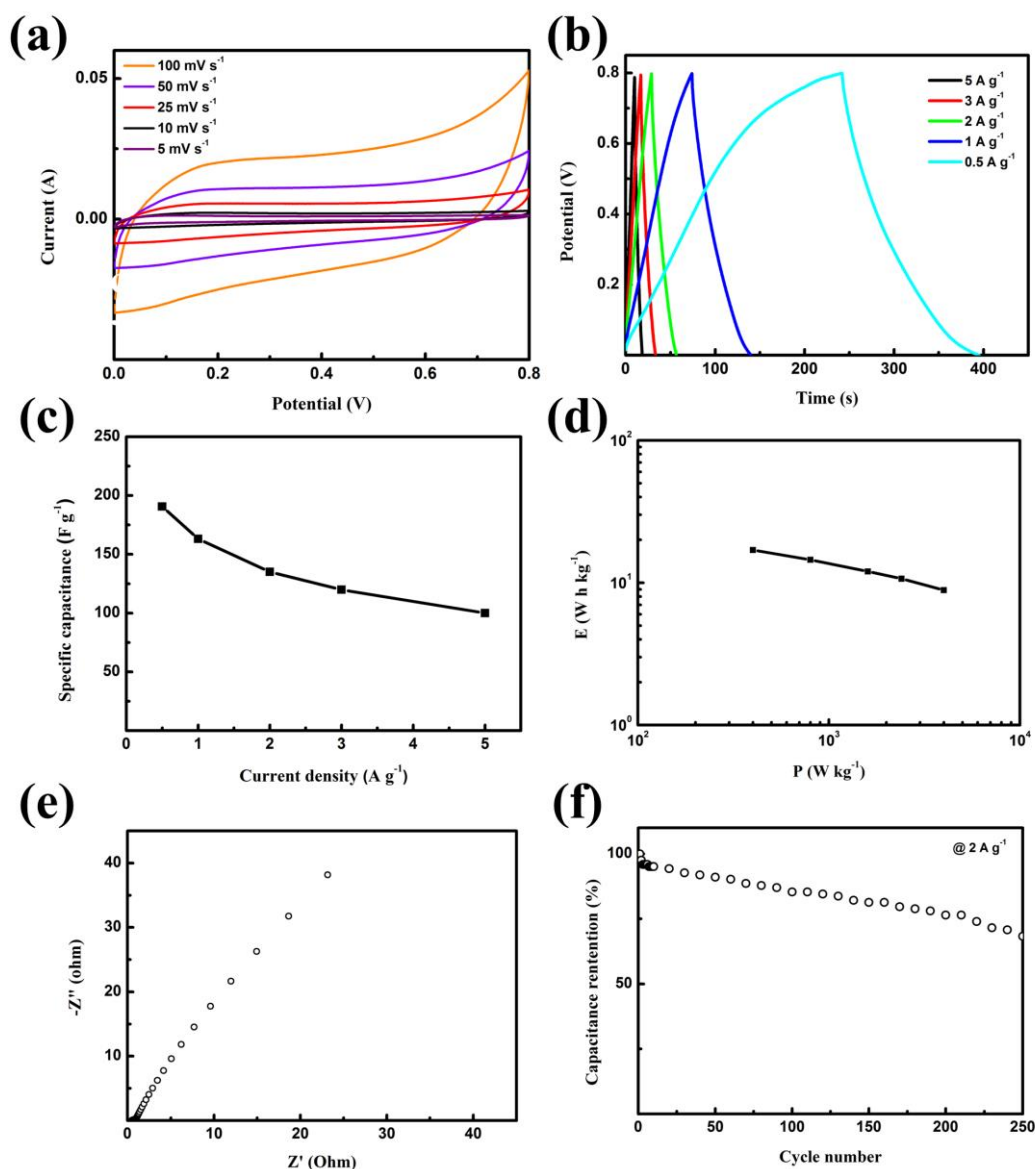
Figure 4. Electrochemical properties of the symmetric supercapacitor. (a) CV curves at different scan rates, (b) GCD curves at different current densities, (c) Specific capacitances calculated at different current densities, (d) Ragone plot, (e) Nyquist plot and (f) cycling stability.

3.3 Electrochemical properties of the supercapacitors in series

The electrochemical properties of the supercapacitors connected in series were studied and the GCD curves was tested at a charge/discharge current of 10 mA, as shown in Fig. 5a. The voltage window of the single device is 0.8 V and the charge/discharge potential of the devices in serial can be multiplied by the number of the supercapacitors. The potential of the three devices assembled in serial achieves 2.4 V. The discharge time increases slowly with the number of devices. The coulombic efficiency of the single supercapacitor is superior. While the charge time of the three devices in serial became larger than that of the single device, which were caused by the discrepancy of each device and the connection method [28]. The digital photograph of the single flexible supercapacitor is shown in Fig. 5b and the circuit for the driving light-emitting diode (LED) lamp is shown in Fig. 5c. The three devices connected in series can light up a red LED.
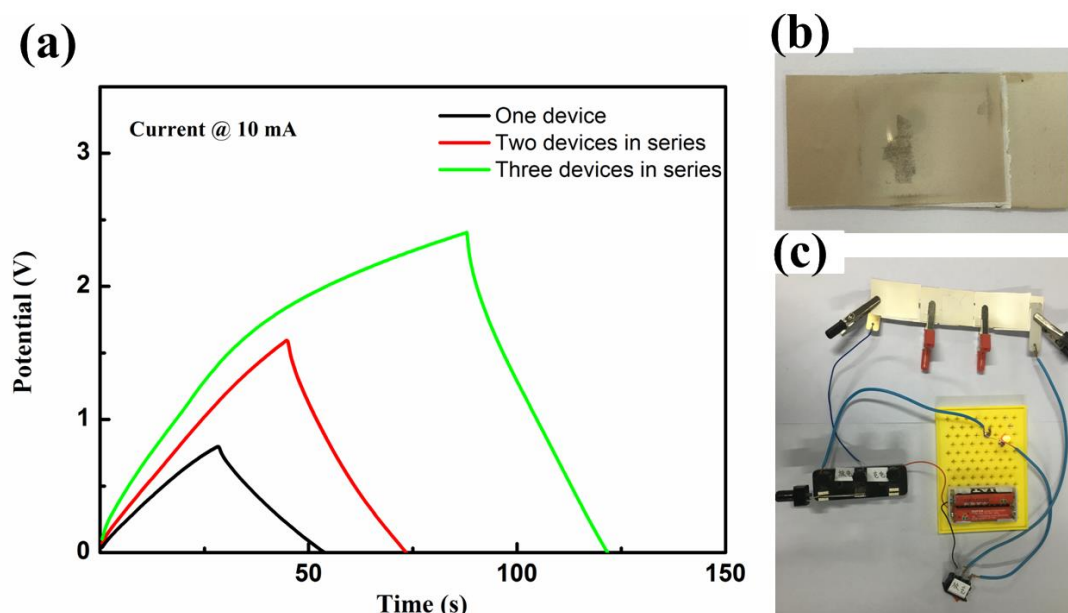
Figure 5. (a) Electrochemical performance of the single device and the devices connected in series, (b) a digital photograph of the all-solid-state flexible supercapacitor, and (c) the three devices connected in series to light up an LED.

4. CONCLUSIONS

In summary, graphene ink was obtained via a grinding method in a ball mill and a supercapacitor electrode was fabricated using the obtained graphene ink and conductive silver ink using a screen printing technology. A flexible supercapacitor was successfully assembled and three devices connected in a series were used to light up a red LED lamp. The maximum specific capacitance of a single device was 190.6 F g^{-1} and the energy density was 16.94 W h kg^{-1} at a power density of 400 W kg^{-1}. A flexible electrode with a facile fabrication method has wide application in energy storage fields and a flexible supercapacitor has great potential for wearable electronics and smart packaging industries.

References

1   X. Peng, L. Peng, C. Wu, Y. Xie, *Chem. Soc. Rev.*, 43 (2014) 3303.
2   L. L. Zhang, X. S. Zhao, *Chem. Soc. Rev.*, 38 (2009) 2520.
3   P. Tamilarasan and S. Ramaprabhu, *Energy*, 51 (2013) 374.
4   Y. J. Kang, B. Kim, H. Chung and W. Kim, *Synthetic M*et., 160 (2010) 2510.
5   S. Wang, B. Pei, X. Zhao and R. A. W. Dryfe, *Nano Energy*, 2 (2013) 530.
6   J. Yang, G. Li, Z. Pan, M. Liu, Y. Hou, Y. Xu, H. Deng, L. Sheng, X. Zhao, Y. Qiu and Y. Zhang, *ACS Appl. Mater. Interfaces*, 7 (2015) 22172.
7   L. Mo, J. Ran, L. Yang, Y. Fang, Q. Zhai and L. Li, *Nanotechnology*, 27 (2016) 065202.
8   Z. Xin, Y. Liu, X. Li, S. Liu, Y. Fang, Y. Deng, C. Bao and L. Li, *Mater. Res. Express*, 4 (2017) 015021.
9   Y. L. Li, Z. Q. Xin, M. J. Cao, et al. A preparation method of flexible supercapacitor electrodes[P], CN106783220A.
10   Y. F. Xu, M. G. Schwab, A. J. Strudwick, I. Hennig, X. L. Feng, Z. S. Wu and K. Müllen, *Adv. Energy Mater.*, (2013) 1.
11   A. Martinez-Olmos, J. Fernandez-Salmeron, N. Lopez-Ruiz, A. Rivadeneyra Torres, L. F. Capitan-Vallvey and A. J. Palma, *Anal. Chem.*, 85 (2013) 11098.
12   S. Cho, M. Kim and J. Jang, *ACS Appl. Mater. Interfaces*, 7 (2015) 10213.
13   S. Zheng, Z. S. Wu, S. Wang, H. Xiao, F. Zhou, C. Sun, X. Bao and H. M. Cheng, *Energy Storage Mater.,* 6 (2017) 70.
14   Y. B. Tan and J. M. Lee, *J. Mater. Chem. A*, 1, 14814 (2013).
15   M. Khan, M. N. Tahir, S. F. Adil, H. U. Khan, M. R. H. Siddiqui, A. A. Al-warthan and W. Tremel, *J. Mater. Chem.* A, 3 (2015) 18753.
16   L. Grande, V. T. Chundi, D. Wei, C. Bower, P. Andrew and T. Ryhänen, *Particuology*, 10 (2012) 1.
17   D. P. Dubal and R. Holze, Energy, 51, 407 (2013).M. Sawangphruk, P. Srimuk, P. Chiochan, T. Sangsri and P. Siwayaprahm, *Carbon*, 50 (2012) 5156.
18   Z. Li, J. Wang, S. Liu, X. Liu and S. Yang, *J. Power Sources*, 196 (2011) 8160.
19   Q. Zheng, Z. Cai, Z. Ma and S. Gong, *ACS Appl. Mater. Interfaces*, 7 (2015) 3263.
20   L. Mao, C. Guan, X. Huang, Q. Ke, Y. Zhang and J. Wang, *Electrochim. Acta*, 196 (2016) 653.
21   X. Peng, D. Q. Li, J. Peng, L. L. Peng, C. Z. Wu and Y. Xie. *Chinese Sci. Bull*., 28-29 (2013) 2886.
22   M. Sawangphruk, P. Srimuk, P. Chiochan, T. Sangsri and P. Siwayaprahm, *Carbon*, 50 (2012) 5156.
23   A. Pramanik, S. Maiti and S. Mahanty, *Dalton T.*, 44 (2015) 14604.
24   Z. Niu, L. Zhang, L. Liu, B. Zhu, H. Dong and X. Chen, *Adv. Mater.*, 25 (2013) 4035.
25   S. Wang, B. Pei, X. Zhao and R. A. W. Dryfe, *Nano Energy*, 2 (2013) 530.
26   M. Wang, D. Duong le, N. T. Mai, S. Kim, Y. Kim, H. Seo, Y. C. Kim, W. Jang, Y. Lee, J. Suhr and J. D. Nam, *ACS Appl. Mater. Interfaces*, 7 (2015) 1348.
27   D. Zhao, C. Chen, Q. Zhang, W. Chen, S. Liu, Q. Wang, Y. Liu, J. Li and H. Yu, *Adv. Energy Mater.*, (2017) 1700739.

28 H. T. Zhang, H. Su, L. Zhang, B. B. Zhang, F. J. Chun, X. Chu, W. D. He and W. Q. Yang. *J. Power Sources*. 331 (2016) 332.